

Pan-cancer analysis and experimental validation reveal UTP4 as a novel biomarker for gastric cancer

DIAO WEI¹⁻³, TIANYU LEI¹⁻³, YUHANG CHE^{2,3} and QINYONG HU¹⁻³

¹Department of Oncology, Renmin Hospital of Wuhan University, Wuhan, Hubei 430060, P.R. China;

²Renmin Hospital of Wuhan Economic and Technological Development Zone, Wuhan, Hubei 430056,

P.R. China; ³Wuhan University Heavy Ion Medicine Center, Wuhan, Hubei 430090, P.R. China

Received September 8, 2025; Accepted January 9, 2026

DOI: 10.3892/mco.2026.2933

Abstract. UTP4 is a critical component of ribosome biogenesis, and its dysregulation may contribute to cancer development. However, the role of UTP4 in cancer remains unclear. The present study comprehensively investigated the expression and prognostic significance of UTP4 across multiple cancers, with a particular focus on gastric cancer (GC). Integrated bioinformatics analysis of public datasets, including The Cancer Genome Atlas, revealed that UTP4 is frequently overexpressed in various tumors and associated with poor prognosis. Further analysis uncovered its correlations with genetic mutations, immune infiltration and immune checkpoint expression. Based on these findings and CRISPR-Cas9 screening predictions, the functional role of UTP4 in GC cells was experimentally validated. The results demonstrated that UTP4 knockdown significantly inhibited cell proliferation, migration and invasion. These findings highlight UTP4 as a novel pan-cancer biomarker and potential therapeutic target, providing a foundation for further clinical investigations.

Introduction

The rising incidence of early-onset cancer has become a critical global health concern, with the age at diagnosis continuously decreasing. Gastric cancer (GC), ranked as the fifth most common malignancy globally, presents substantial clinical challenges due to its frequently hidden early symptoms and the absence of effective diagnostic tools (1,2). Consequently, numerous patients are diagnosed at an advanced stage, resulting in a poor five-year survival rate of ~20-30% (3,4).

Despite therapeutic progress, including surgery, chemotherapy, radiotherapy and immunotherapy, the management of GC remains challenging. Tumor heterogeneity, a complex tumor microenvironment (TME), and frequent therapeutic resistance often result in recurrence and unfavorable outcomes (5-9). Therefore, identifying biomarkers that accurately predict therapeutic efficacy in GC is imperative.

Recent studies emphasize the critical role of ribosome biogenesis (RB) in cancer development. This complex process involves the synthesis, modification, and assembly of ribosomal RNA (rRNA). RB is fundamental to cellular function and is tightly regulated. UTP4, also known as CIRH1A, functions as a ribosomal RNA processing factor involved in the biosynthesis of the small ribosomal subunit (10). Elevated UTP4 expression levels have been closely associated with tumor growth and disease progression across multiple cancer types.

For instance, reduced UTP4 expression has been shown to significantly inhibit ribosome synthesis (11). Additionally, mutations in the UTP4 gene are linked to North American Indian Childhood Cirrhosis (NAIC), further highlighting its essential role in RB (12,13). In colorectal cancer (CRC) cells, RNA interference (RNAi)-mediated suppression of UTP4 notably decreased cell proliferation and promoted apoptosis (14). Similarly, in gliomas, high levels of UTP4 have been strongly correlated with rapid tumor progression and poor clinical outcomes (15). These collective findings suggest that UTP4 serves as a pivotal regulator in RB and potentially contributes to cancer progression.

The present study aims to evaluate UTP4 as a pan-cancer prognostic biomarker and to validate its biological functions in GC. By utilizing multi-omics data from TCGA and other databases, the expression patterns of UTP4 were comprehensively analyzed across multiple cancer types and its associations with patient prognosis were examined. Additionally, through in vitro experiments, the influence of UTP4 on GC cell proliferation, migration and invasion was explored. The present findings offer novel insights into UTP4's role in cancer biology and underscore its potential as a prognostic biomarker and therapeutic target for GC.

Correspondence to: Professor Qinyong Hu, Department of Oncology, Renmin Hospital of Wuhan University, 99 Zhangzhidong Road, Wuchang, Wuhan, Hubei 430060, P.R. China
E-mail: rm001223@whu.edu.cn

Key words: UTP4, gastric cancer, biomarker, single-cell spatial transcriptomics, multi-omics

Materials and methods

Data collection. RNA sequencing data and clinical details regarding UTP4 were retrieved from The Cancer

Genome Atlas (TCGA) database (<http://cancergenome.nih.gov/>). Protein expression data were obtained from the UALCAN database (<http://ualcan.path.uab.edu/index.html>). Additionally, whole-genome CRISPR-Cas9 screening data were downloaded from the DepMap portal (<https://depmap.org/portal/download/>).

Genomic and protein alterations of UTP4 in pan-cancer. RNA sequencing and clinical data covering 33 tumor types were carefully analyzed after download from the TCGA database. Expression levels in transcripts per million (TPM) were converted using log₂ transformation for accuracy. Differences in UTP4 expression across tumor types were further analyzed by constructing boxplots and paired plots in R (version 4.2.1) using packages such as ggplot2 (version 3.3.6), stats (version 4.2.1), and car (version 3.1-0). The Tumor Immune Estimation Resource version 2 (TIMER2.0; <http://timer.cistrome.org/>) was also used to compare UTP4 expression between tumor and normal tissues.

The UALCAN platform (<http://ualcan.path.uab.edu/index.html>) was utilized for additional analyses. The proteomics module within UALCAN allowed comparisons of UTP4 protein expression between tumor and normal tissues, as well as analyses of its association with clinical characteristics, including cancer stage.

UTP4 expression at single-cell spatial transcriptomics level. To further validate differences in UTP4 expression in cancer and examine its gene expression profiles in specific cell types, the Sparkle database (<https://grswsci.top/>) was employed. The Spatial Transcriptomics module was selected, and five datasets were analyzed, namely ‘CESC: Human_Cervical_Cancer (10x database)’, ‘GIST2: GSE203612-GSM6177609’, ‘HNSC2: GSE181300-GSM5494476_HNSCC201125T05’, ‘KIRC2: GSE175540-GSM5924030_ffpe_c_2’, and ‘CRC2: IntestineCancer_10x_FFPE (10x database)’, to explore differences in UTP4 expression at single-cell resolution within spatial transcriptomic contexts.

Prognostic and diagnostic value analysis. RNA sequencing data and clinical information for the 33 tumor types were standardized and analyzed for prognostic significance. Using the R ‘survival’ package, Kaplan-Meier survival curves were constructed, proportional hazards assumption tests were performed, and survival regression models were fitted.

Receiver operating characteristic (ROC) curve analysis was conducted using the timeROC package (version 0.4) to evaluate diagnostic performance. The area under the ROC curve (AUC) values, ranging from 0.5 to 1, were assessed to determine diagnostic capability, with higher AUC values indicating superior diagnostic accuracy (16).

UTP4 gene alteration analysis. To investigate UTP4 gene alterations across different cancers, the cBioPortal platform (<https://www.cbioportal.org/>) was utilized, an interactive tool designed for analyzing multidimensional cancer genomic datasets. The study cohort was selected from the ‘TCGA PanCancer Atlas Studies’, and the UTP4 gene was queried using cBioPortal’s module to obtain relevant mutation information. The ‘Cancer Types Summary’ module provided an overview of

mutation frequencies and types associated with UTP4 across various cancers. Additionally, the ‘Mutations’ module offered detailed insights into mutation sites, counts, and types within the UTP4 gene. Mutation data were subsequently visualized using cBioPortal’s visualization tools. To further analyze the mutational landscape, the ‘Mutation Effect-Expression’ module of the Sparkle database (<https://grswsci.top/>) was employed. This database enabled analysis of UTP4 mutation types and single nucleotide variations (SNVs), revealing potential roles for UTP4 gene alterations in cancer progression.

Immune-related analysis. Multiple databases were used to investigate the relationship between UTP4 and immune processes. Initially, immune infiltration associated with UTP4 expression across various tumors was analyzed using the Xiantao Academy (www.xiantaozi.com). Subsequently, the Sparkle database (<https://grswsci.top/>) was utilized to examine associations between UTP4 expression and the tumor immune microenvironment, including immune cells specifically in GC. Finally, correlations between pan-cancer UTP4 expression and tumor stemness, as well as immune checkpoints, were explored using the SangerBox tool (<http://sangerbox.com/home.html>).

Protein-protein interaction network and enrichment analysis. The protein interaction network involving UTP4 was obtained from the STRING database (<https://string-db.org/>) (17). Next, the top 100 genes correlated with UTP4 expression were retrieved from GEPIA2.0 (<http://timer.cistrome.org/>) (18). Utilizing the ‘clusterProfiler (version 4.4.4)’ package in R, enrichment analysis was performed on the top 10 correlated genes. This allowed the identification of crucial phenotypes and signaling pathways involving UTP4 across pan-cancer contexts. Additionally, Pearson correlations between UTP4 expression z-scores and GSEA scores for 14 tumor states were analyzed using the ‘Pathway Analysis-Activity Score’ template provided by the Sparkle database (<https://grswsci.top/>) (19).

Univariate Cox regression analysis in pan-cancer and multivariate cox regression analysis in GC. The proportional hazards assumption was verified using the ‘survival’ package in R, followed by univariate Cox regression analysis conducted across various tumors. Specifically focusing on GC, multivariate Cox proportional hazards regression analysis was performed to assess the independent prognostic significance of UTP4, adjusting for clinical variables including age, sex and tumor stage. The results were illustrated through forest plots displaying hazard ratios (HRs), 95% confidence intervals (CIs), and P-values for UTP4 and other clinical factors.

Bayesian colocalization analysis. Mendelian colocalization analysis, a statistical method used to investigate genetic associations with diseases across multiple phenotypes, was employed to identify shared genetic factors. To explore genetic associations of UTP4 in pan-cancer and GC contexts, datasets for pan-cancer (ieu-b-4966) and GC (ebi-a-GCST90018629) were downloaded from the OpenGWAS database. Colocalization analysis was conducted using the ‘coloc’ package. Results were visualized through the ‘locuscompare’ function within the ‘locuscompare’ package and the ‘stack_assoc_plot’ function from the ‘gassocplot2’ package. A posterior probability

(PP.H4.abf) greater than 80% was set as the threshold indicating robust evidence of colocalization (20).

Dependency score of UTP4 in various tumor cell lines. Genome-wide CRISPR-Cas9 screening data were obtained from the DepMap portal (<https://depmap.org/portal/download/>). This dataset includes dependency scores for candidate genes across numerous cancer cell lines, calculated using the CERES algorithm. The CERES dependency scores for UTP4, which were scaled such that 0 indicates a non-essential gene and -1 denotes the median dependency of core essential genes, were specifically analyzed. The 200 cell lines exhibiting the most negative UTP4 dependency scores were selected and visualized using bar plots.

Cell culture and transfection. The human normal gastric epithelial cell line GES-1 and GC cell lines AGS and MKN-45 were purchased from Sai Bai Kang (Shanghai) Biotechnology Co., Ltd. Cells were cultured in medium containing 5% fetal bovine serum (Gibco; Thermo Fisher Scientific, Inc.) at 37°C with 5% CO₂. Cells in optimal growth conditions were transfected with CRISPR-Cas9 small guide RNA (sgRNA) lentiviral vectors. A total of three distinct sgRNAs were designed against the human UTP4 gene. Their RNA guide sequences (5'-3') are as follows: sgRNA#1: AUGCCUUUGGAGGACCUAAU; sgRNA#2: CGUCAGCAUUAGCGAUGAGA; and sgRNA#3: GUAGCCCGAGACUCAUGACC.

The knockdown efficiency of all three sgRNAs was initially evaluated by reverse transcription-quantitative PCR (RT-qPCR). sgRNA#2 showed the strongest and most consistent reduction in UTP4 mRNA levels and was therefore chosen to generate stable knockdown cell pools for all subsequent functional experiments. A custom non-targeting control (NTC) sgRNA was included in parallel to account for potential non-specific effects associated with lentiviral transduction and Cas9 activity. Its RNA guide sequence is: GGCAGCGAGAUAAACUUGACUC. All sgRNA lentiviral vectors were supplied by Shenggong Bioengineering (Shanghai) Co., Ltd. The initial qPCR screening data assessing the knockdown efficiency of the three sgRNAs are provided in Fig. S1 and Table SIII.

Cell Counting Kit-8 (CCK-8) assay. Cell viability following sgRNA transfection was measured using the CCK-8 from Shanghai Taosu Biotechnology Co., Ltd. Transfected cells were seeded into 96-well plates at a density of 1x10³ cells per well and incubated overnight at 37°C. At 0, 1, 2, and 3 days, 10 µl of CCK-8 solution was added to each well, and absorbance was measured at a wavelength of 450 nm.

RT-qPCR. Total RNA was extracted from cells using TRIzol Universal RNA extraction reagent according to the manufacturer's protocol. RT-qPCR were performed using the Vazyme genomic RT-qPCR kit and an ABI 7900HT Fast Real-Time PCR System (Applied Biosystems; Thermo Fisher Scientific, Inc.). The thermocycling conditions for PCR amplification were as follows: Initial denaturation at 95°C for 30 sec; 40 cycles of denaturation at 95°C for 10 sec, annealing at 60°C for 30 sec, and extension at 72°C for 30 sec. Quantification was performed using the 2^{-ΔΔC_q} method (21). Each experiment

was repeated three times. The primer sequences used were as follows: UTP4 forward, 5'-AGGTCCATCGAGTACGTT TCT-3' and reverse, 5'-CACAGTGCCATCTGTTCGTG-3'. GAPDH was used as an endogenous control for normalization. The primer sequences for GAPDH were as follows: forward, 5'-GAAGGTGAAGGTCGGAGTC-3' and reverse, 5'-GAA GATGGTGATGGGATTTC-3'.

Wound healing assay. Prior to the scratch assay, cells were serum-starved in medium containing 0.5% FBS for 12 h to suppress cell proliferation. A baseline was drawn horizontally at the bottom of each well in a six-well plate for reference. Once cells reached near-confluence, a sterile pipette tip was gently used to scratch a straight line along the baseline, creating a wound. Images of the initial wound state were immediately captured under a light microscope, and its width was recorded. After 48 h, images of the wound area were captured again. The wound area was precisely measured using ImageJ software (version 1.53t; National Institutes of Health) to assess cell migration rates and wound closure efficiency.

Apoptosis assay. Cells were cultured in six-well plates to an appropriate density. Cell apoptosis was assessed following the manufacturer's protocol using the Annexin V-AF488/PI Apoptosis Detection Kit (BioLegend-Shanghai Yaji Biotechnology Co., Ltd.). The number of apoptotic cells was quantitatively determined using a BD LSRFortessa flow cytometer (BD Biosciences) and analyzed with BD FACSDiva software (version 9.0; BD Biosciences).

Statistical analysis. Statistical analyses were performed using R (version 4.3.0) and GraphPad Prism (version 10.3.0), with visualization and specific tests conducted via R packages (ggplot2, survminer, pheatmap, timeROC). A two-sided P<0.05 was considered to indicate a statistically significant difference.

For public omics and clinical data, continuous variables are presented as the mean ± SD or median (IQR). Group comparisons used paired/independent t-tests, one-way ANOVA (with Tukey's post hoc test), or Kaplan-Meier analysis (log-rank test). The independent prognostic value of UTP4 was assessed by Cox proportional hazards regression (assumption verified via Schoenfeld residuals). Diagnostic performance was evaluated with time-dependent ROC curves. Correlations were calculated using Pearson's coefficient. Functional enrichment (GO/KEGG) was analyzed with the clusterProfiler package (FDR-adjusted).

For *in vitro* data, results from ≥3 independent replicates are shown as mean ± SD. Comparisons used the independent t-test (two groups) or two-way ANOVA with Tukey's post hoc tests, as indicated.

Results

Abnormal expression of UTP4 in various tumors and normal tissues. To examine differential UTP4 expression across cancer types, RNA sequencing data from the TCGA database were analyzed. UTP4 was significantly upregulated in several cancers, including cholangiocarcinoma (CHOL), colon adenocarcinoma (COAD), esophageal cancer (ESCA), head

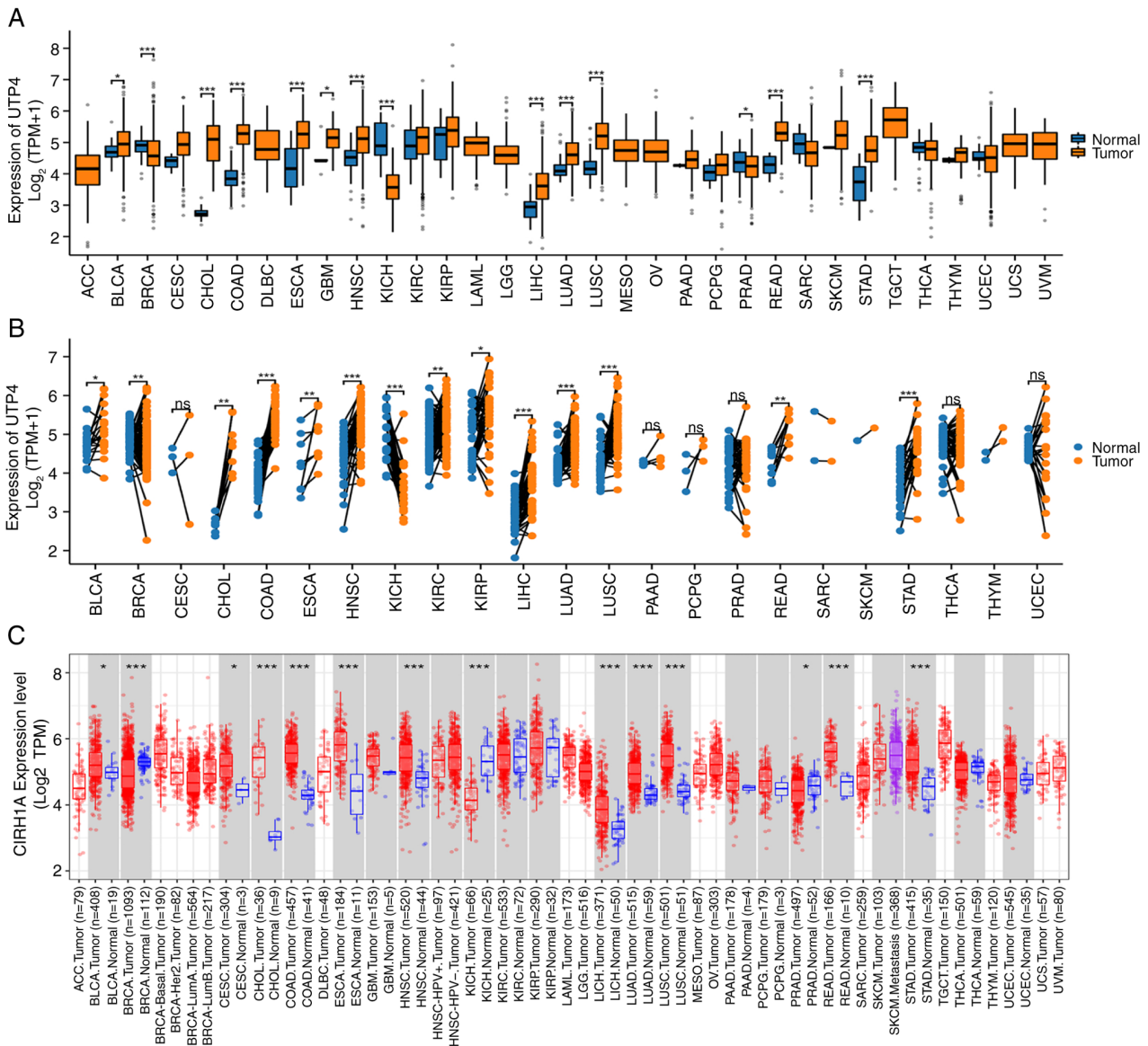


Figure 1. (A) UTP4 expression across pan-cancer types based on the TCGA dataset. (B) Comparison of UTP4 expression between paired tumor and normal samples from TCGA. (C) UTP4 expression across pan-cancer types using the TIMER2.0 database. * $P < 0.05$, ** $P < 0.01$ and *** $P < 0.001$. TCGA, The Cancer Genome Atlas; ns, not significant. ACC, adenoid cystic carcinoma; BLCA, bladder urothelial carcinoma; BRCA, breast cancer; CESC, cervical squamous cell carcinoma; CHOL, cholangiocarcinoma; COAD, colon adenocarcinoma; DLBC, diffuse large B-cell lymphoma; ESCA, esophageal carcinoma; GBM, glioblastoma multiforme; HNSC, head and neck cancer; KICH, kidney chromophobe; KIRC, kidney renal clear cell carcinoma; KIRP, kidney renal papillary carcinoma; LAML, acute myeloid leukemia; LGG, low-grade glioma; LIHC, liver hepatocellular carcinoma; LUAD, lung adenocarcinoma; LUSC, lung squamous cell carcinoma; MESO, mesothelioma; OV, ovarian cancer; PAAD, pancreatic adenocarcinoma; PCPG, pheochromocytoma; PRAD, prostate adenocarcinoma; READ, rectum adenocarcinoma; SARC, sarcoma; SKCM, skin cutaneous melanoma; STAD, stomach adenocarcinoma; TGCT, tenosynovial giant cell tumor; THCA, thyroid carcinoma; THYM, thymoma; UCEC, uterine corpus endometrial carcinoma; UCS, uterine carcinosarcoma; UVM, uveal melanoma.

and neck cancer (HNSC), hepatocellular carcinoma (LIHC), lung adenocarcinoma (LUAD), lung squamous cell carcinoma (LUSC), rectal adenocarcinoma (READ), stomach adenocarcinoma (STAD), bladder cancer (BLCA) and glioblastoma (GBM) ($P < 0.05$) (Fig. 1A). These findings suggest that UTP4 may play an important role in the initiation and progression of multiple malignancies. Conversely, UTP4 expression was significantly decreased in breast cancer (BRCA), kidney chromophobe (KICH) and prostate cancer (PRAD) ($P < 0.05$; Fig. 1A). A follow-up analysis using cancer-paired samples further supported these results. Pronounced differences in UTP4 expression were observed across the corresponding

tumor types, consistent with the initial findings (Fig. 1B). Additional validation using the TIMER2.0 database confirmed similar expression patterns. Although the difference in UTP4 expression in GBM did not reach statistical significance, other cancer types exhibited expression trends consistent with the TCGA analysis. Notably, cervical cancer (CESC) showed significant upregulation of UTP4 ($P < 0.05$; Fig. 1C).

Differential expression of UTP4 at the protein level. To further characterize UTP4 expression at the protein level, proteomic data from the UALCAN database were analyzed. UTP4 protein levels were significantly elevated in multiple

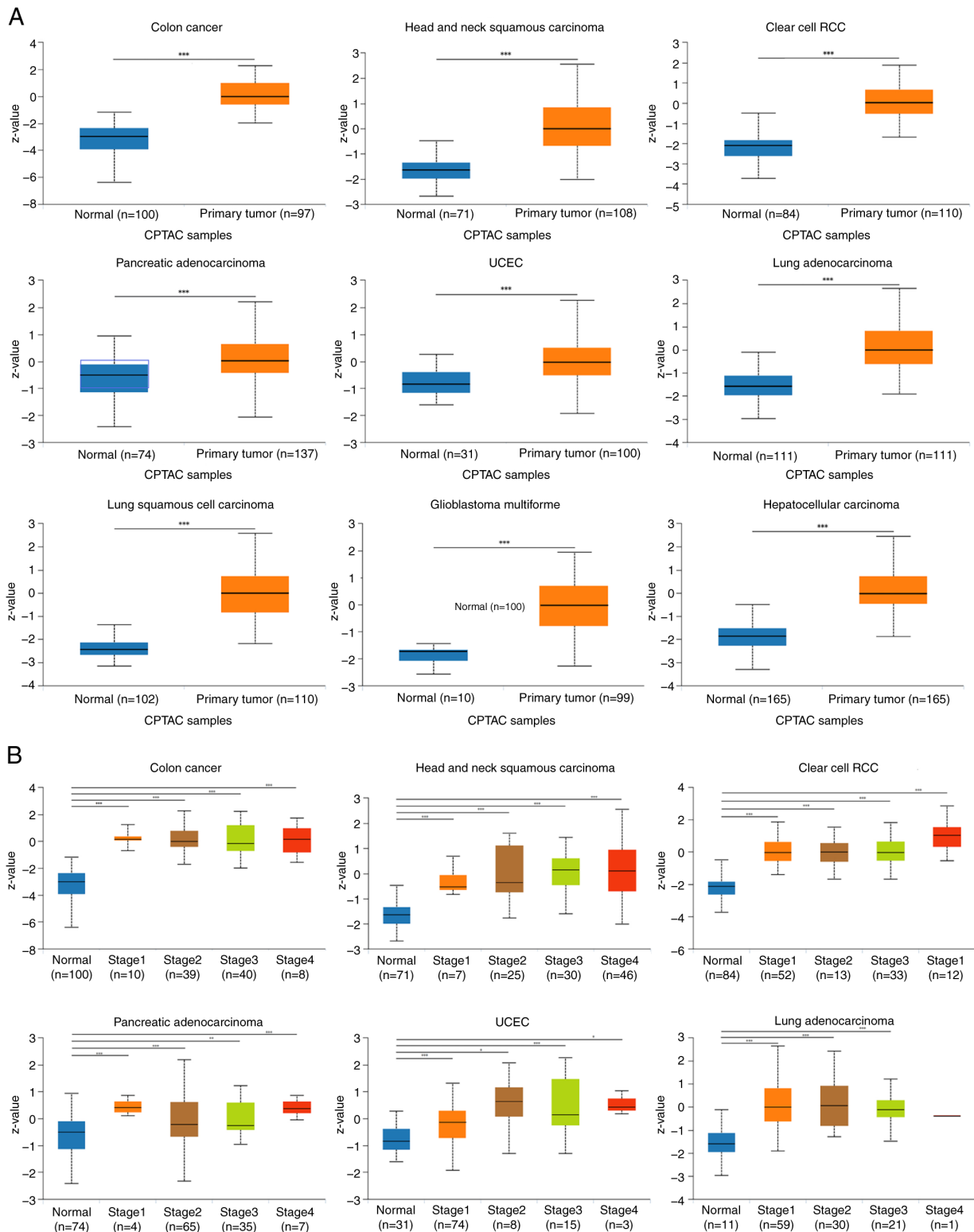


Figure 2. (A) UTP4 protein expression in COAD, HNSC, KIRC, PAAD, UCEC, LUAD, LUSC, glioblastoma multiforme and liver hepatocellular carcinoma from the UALCAN database. (B) Differential UTP4 expression across pathological stages in COAD, HNSC, KIRC, PAAD, UCEC and LUAD. * $P < 0.05$, ** $P < 0.01$ and *** $P < 0.001$. COAD, colon adenocarcinoma; HNSC, head and neck cancer; KIRC, kidney renal clear cell carcinoma; PAAD, pancreatic adenocarcinoma; UCEC, uterine corpus endometrial carcinoma; LUAD, lung adenocarcinoma; RCC, renal cell carcinoma; ns, not significant.

cancer types, including COAD, HNSC, kidney renal clear cell carcinoma (KIRC), pancreatic adenocarcinoma (PAAD), endometrial carcinoma (UCEC), LUAD, LUSC, GBM and LIHC ($P < 0.05$; Fig. 2A). These findings reinforce the hypothesis that UTP4 may contribute to tumor progression.

Moreover, UTP4 protein expression varied significantly across pathological stages in COAD, HNSC, KIRC, PAAD, UCEC and lung cancer ($P < 0.05$; Fig. 2B). This stage-dependent variation suggests that UTP4 overexpression is closely linked to tumor development rather than being an isolated

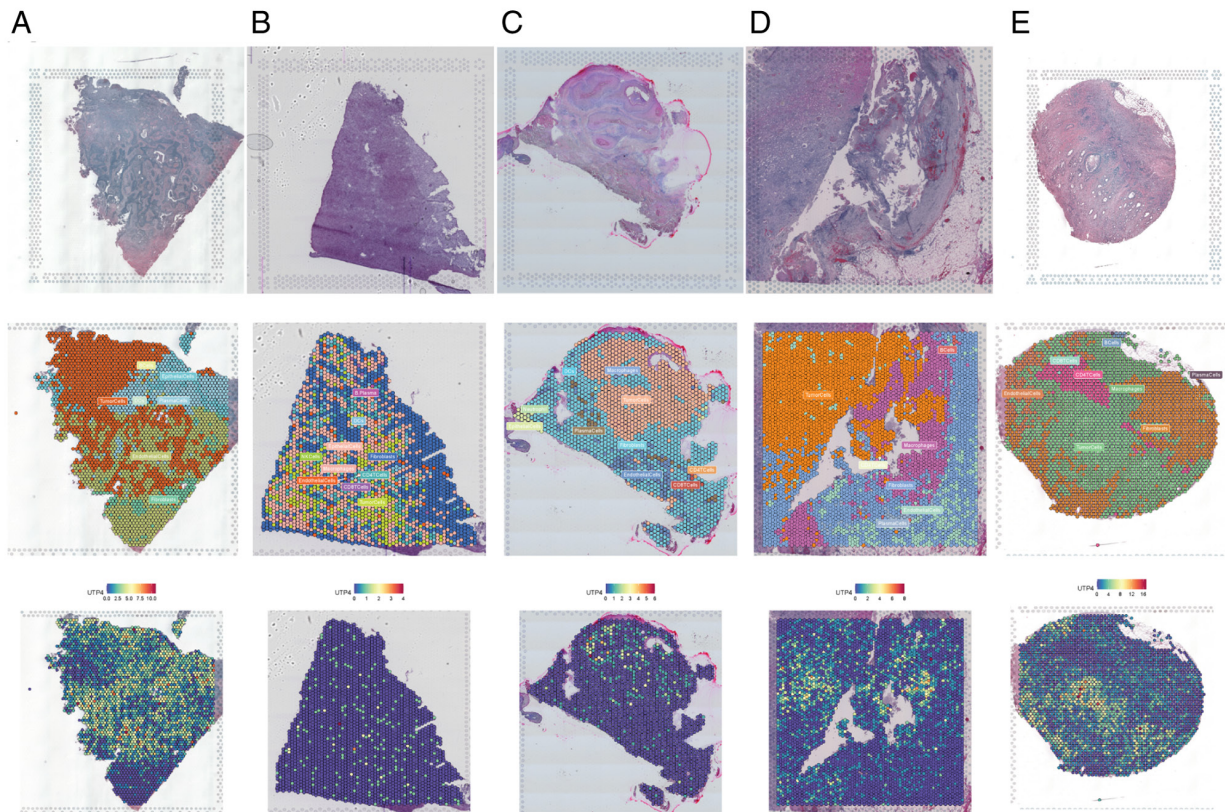


Figure 3. (A-E) Tissue images displaying UTP4 expression in cutaneous squamous cell carcinoma, gastrointestinal stromal tumor, head and neck squamous cell carcinoma, clear cell renal cell carcinoma and colorectal cancer datasets, respectively. Each shows the predominant cellular composition per spot after spatial transcriptomic deconvolution and UTP4 localization within spatial transcriptomes.

molecular event, supporting its potential role in cancer progression.

Differential expression of UTP4 in single cells. Single-cell spatial transcriptomic analysis was conducted to precisely evaluate UTP4 expression differences among various cancers and cell types (22). This approach allowed detailed exploration of UTP4 expression in specific cellular populations (23,24). The results demonstrated that in human cervical squamous cell carcinoma samples (Human_Cervical_Cancer), UTP4 expression was mainly detected in tumor and epithelial cells (Fig. 3A). Similarly, gastric stromal tumor (GSE203612-GSM6177609) samples showed predominant UTP4 expression in tumor and epithelial cells (Fig. 3B). In head and neck squamous cell carcinoma (GSE181300-GSM5494476_HNSCC201125T05), UTP4 expression was concentrated predominantly in tumor cells (Fig. 3C). In clear cell renal cell carcinoma (GSE175540-GSM5924030_ffpe_c_2) samples, UTP4 was expressed not only in tumor cells but also in macrophages (Fig. 3D). In CRC (IntestineCancer_10x_FFPE) samples, UTP4 expression was primarily localized to tumor and epithelial cells (Fig. 3E). These single-cell spatial transcriptomics findings highlight that UTP4 is predominantly expressed in tumor and epithelial cells in various tumor tissues, suggesting its critical involvement across multiple cancer types.

Prognostic and diagnostic value of UTP4 in pan-cancer. A comprehensive survival analysis was conducted to evaluate the prognostic significance of UTP4. Elevated

UTP4 expression significantly correlated with poor prognosis in multiple cancers, including ACC ($P=0.021$), HNSC ($P=0.008$), GBMLGG ($P<0.001$), LUAD ($P=0.010$), LGG ($P=0.015$), LIHC ($P=0.036$), PAAD ($P=0.025$), SARC ($P=0.048$), STAD ($P=0.023$) and OSCC ($P=0.038$) (Fig. 4A). These results imply that UTP4 may be a robust indicator of adverse outcomes, underscoring its importance in cancer progression and patient survival. By contrast, high UTP4 expression correlated with favorable prognosis in KIRC ($P<0.001$) (Fig. 4A). Furthermore, ROC curve analysis evaluated the diagnostic accuracy of UTP4. UTP4 demonstrated strong diagnostic performance in KICH (AUC=0.959), STAD (AUC=0.894), LIHC (AUC=0.823) and OSCC (AUC=0.810) (Fig. 4B), and moderate diagnostic ability in HNSC (AUC=0.787), GBMLGG (AUC=0.630), LUAD (AUC=0.795), and PAAD (AUC=0.682) (Fig. 4B). Analysis of survival rates by sex showed that the association between UTP4 expression levels and prognosis was more significant in females (Fig. 4C). Notably, although UTP4 expression was significantly associated with overall survival (OS), it showed no statistically significant correlation with the disease-free interval (DFI) ($P=0.39$; Fig. S2). This discrepancy suggests that high expression of UTP4 may not directly drive early tumor recurrence but instead predominantly influences disease progression after recurrence. These findings emphasize the significant prognostic and diagnostic relevance of UTP4 across various cancer types. Collectively, the results support the utility of UTP4 as a potential biomarker

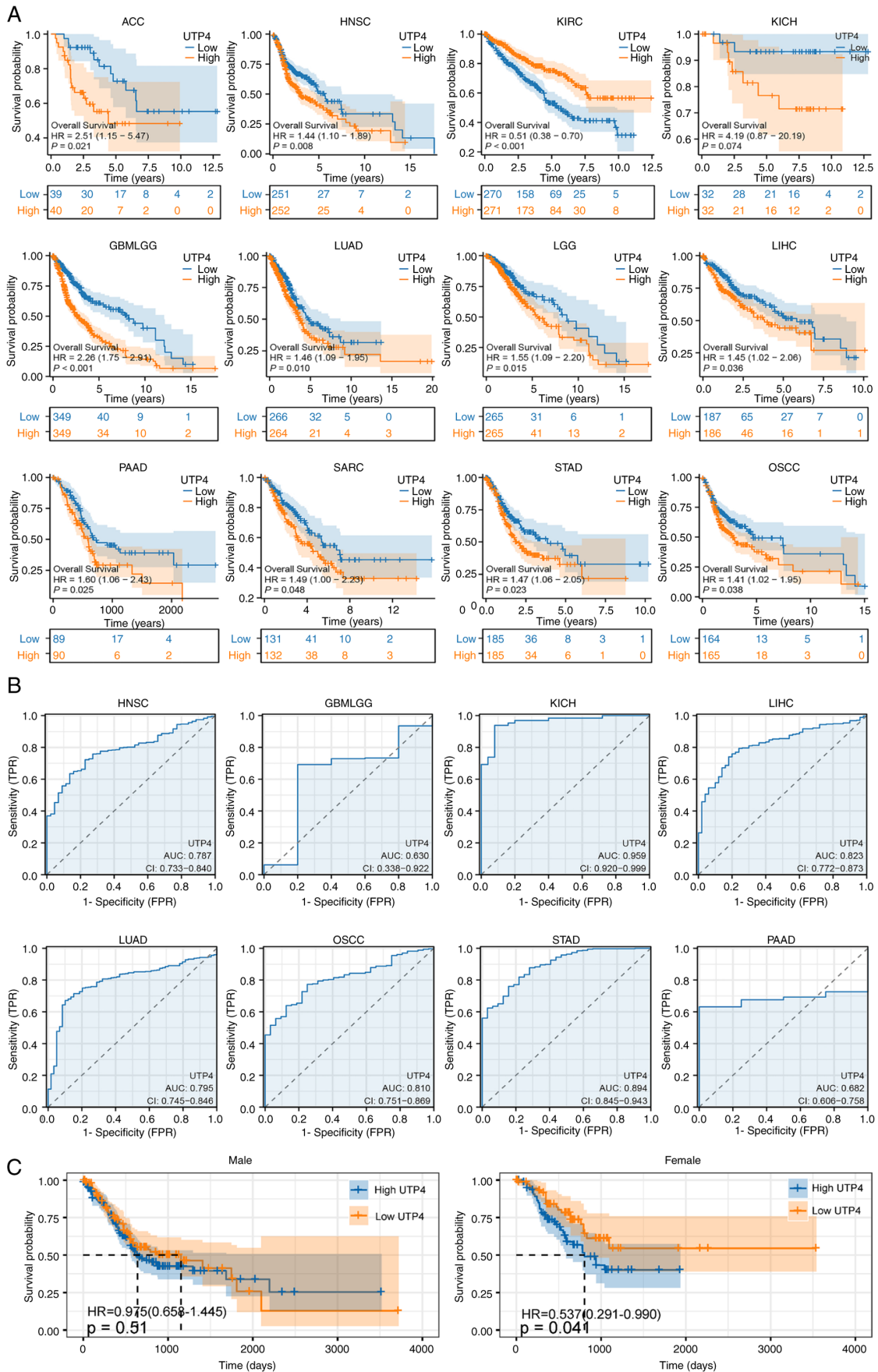


Figure 4. (A) Overall survival analysis of UTP4 using TCGA data. (B) ROC curves for UTP4 based on TCGA data. (C) Comparison of overall survival by sex regarding UTP4 expression based on TCGA data. TCGA, The Cancer Genome Atlas; ACC, adenoid cystic carcinoma; HNSC, head and neck cancer; KIRC, kidney renal clear cell carcinoma; KICH, kidney chromophobe; GBMLGG, glioblastoma and lower-grade glioma; LUAD, lung adenocarcinoma; LGG, low-grade glioma; LIHC, liver hepatocellular carcinoma; PAAD, pancreatic adenocarcinoma; SARC, sarcoma; STAD, stomach adenocarcinoma; OSCC, oral squamous cell carcinoma.

and provide a basis for developing cancer diagnostic and prognostic assessment tools.

Mutation landscape of UTP4. To improve understanding of the mutational characteristics of UTP4 across different cancers, detailed analyses were conducted. Significant variations in UTP4 mutation frequencies and types were observed among cancer types. High mutation frequencies occurred in UCEC (mutation 4.35%, amplification 0.19%, deep deletion 0.95%), BLCA (mutation 0.97%, amplification 1.95%, deep deletion 0.73%, multiple alterations 0.24%), ESAD (mutation 1.65%, amplification 1.65%, deep deletion 0.55%), PRAD (amplification 0.4%, deep deletion 2.63%), CHOL (amplification 2.78%), COADREAD (mutation 2.69%), OV (amplification 0.34%, deep deletion 2.23%), SKCM (mutation 2.03%, amplification 0.23%), BRCA (mutation 0.55%, amplification 0.18%, deep deletion 1.38%), DLBC (deep deletion 2.08%), and STAD (mutation 0.91%, amplification 0.23%, deep deletion 0.68%) (Table SI, Fig. 5A). Further analysis using cBioPortal identified R328Q and P593L/A as the most frequent mutation sites in UTP4. These mutations appeared in multiple cancers and were each supported by at least three samples (Fig. 5B). Statistical evaluation revealed that missense mutations predominated in UTP4, followed by nonsense mutations, while SNVs were mainly single nucleotide polymorphisms (SNPs) (25,26) (Fig. 5C). These findings indicate that UTP4 mutations vary significantly across cancers, suggesting diverse functional roles. Different mutation types might influence UTP4 functionality, potentially affecting cancer initiation and progression. For instance, missense mutations may alter UTP4 protein structure and function, disrupting RB and cancer cell proliferation; nonsense mutations may result in premature termination of UTP4 proteins and loss of function; and SNV-type SNPs may affect the regulation of UTP4 gene expression.

Relationship between UTP4 and immune cells and microorganisms in the TME. Associations between UTP4 expression, immune cells and microorganisms within the TME were further explored. UTP4 expression negatively correlated with most immune cells across pan-cancer analyses, indicating its potential role in inhibiting immune cell infiltration or function. However, positive correlations were noted with specific immune cell subsets, such as T helper cells, central memory T cells and Th2 cells (Fig. 6A). Moreover, UTP4 expression exhibited significant correlations with various microorganisms in the TME. Specifically, in STAD and COAD, UTP4 positively correlated with most microorganisms; in ESCA, it showed negative correlations; in READ and HNSC, both positive and negative correlations were observed (Fig. 6B). These results reflect the complex functional roles of UTP4 across cancers. In GC specifically, elevated UTP4 expression negatively correlated with infiltration of most immune cells but positively correlated with particular immune subsets, including Common lymphoid progenitor_XCELL, T cells CD4+ Th2_XCELL, and T cells CD4+ Th1_XCELL (Fig. 6C). Thus, UTP4 may regulate immune responses and microbial composition in the TME, influencing cancer progression and patient prognosis.

Correlation analysis of UTP4 with tumor stemness and immune checkpoints. Tumor stemness refers to the stem cell-like capacity of tumor cells for self-renewal and differentiation, enabling aggressive proliferation and metastasis (27,28). Tumor stem cells significantly contribute to tumor recurrence and therapy resistance (29). To investigate the role of UTP4 in tumor stemness, correlations between UTP4 expression and tumor mutational burden (TMB) and microsatellite instability (MSI) were analyzed. UTP4 expression positively correlated with TMB in KIRC, UVM, BRCA, HNSC, LUSC, MESO, LGG, CESC, STES, PAAD, OV, READ, GBMLGG, LIHC, GBM, PRAD, DLBC, KIPAN, ACC, SARC, LUAD, STAD, UCS, KIRP and UCEC (Fig. 7A). Similarly, UTP4 expression positively correlated with MSI in LUSC, OV, BRCA, KIRP, BLCA, STES, KIRC, CESC, PAAD, UCS, GBM, LIHC, STAD, SARC, SKCM, UCEC, UVM and CHOL (Fig. 7B). Immune checkpoint molecules are crucial for tumor immune evasion. High UTP4 expression was significantly correlated with immune checkpoint molecules in multiple cancers, including DLBC, OV, KICH, PAAD, BLCA, BRCA, PCPG, PRAD, UCEC, UVM, LIHC, KIPAN, KIRC, THCA, THYM, HNSC, KIRP, LUSC and GBMLGG (Fig. 7C). These results indicate that UTP4 may influence cancer progression and metastasis by regulating tumor stemness, mutation burden and immune checkpoint expression.

Enrichment analysis of UTP4-related genes and correlation analysis of 14 tumor states in GC. To clarify the molecular mechanisms of UTP4 in cancer, enrichment analysis of UTP4-associated genes was performed. Firstly, a protein-protein interaction network involving 11 proteins related to UTP4 was obtained from the STRING database (Fig. 8A). Subsequently, using GEPIA2.0, the top 100 genes co-expressed with UTP4 were identified (Table SII). Among these, the top 10 genes, including NIP7, CIAPIN1 and SF3B3, exhibited strong pan-cancer correlations with UTP4, illustrated by scatter plots (Fig. 8B). GO and KEGG enrichment analyses (Fig. 8C and D) revealed significant involvement of UTP4 in pathways such as RB, RNA processing, and ribonucleoprotein particle assembly, highlighting its essential role in cellular functions. RB is critical for cellular protein synthesis and normal cellular operations (30,31). UTP4's participation suggests roles in various stages of ribosome assembly, potentially supporting rapid cancer cell proliferation. GO analysis results included biological processes (BP), cellular components (CC), and molecular functions (MF). The BP and CC analyses indicated that UTP4 is involved in pre-ribosome assembly and biogenesis, processes essential for efficient protein synthesis in cancer cells. Additionally, CC analysis suggested that UTP4 might participate in the formation and regulation of ribonucleoprotein granules, which influence mRNA storage and translation. Dysregulated ribonucleoprotein granules could disrupt gene expression control, thereby promoting cancer development (32). BP results also indicated that UTP4 might exhibit catalytic functions, particularly ATP-dependent RNA-related activities. Abnormal RNA processing and modification due to altered UTP4 activity may disrupt RNA metabolism, consequently supporting cancer cell proliferation and survival.

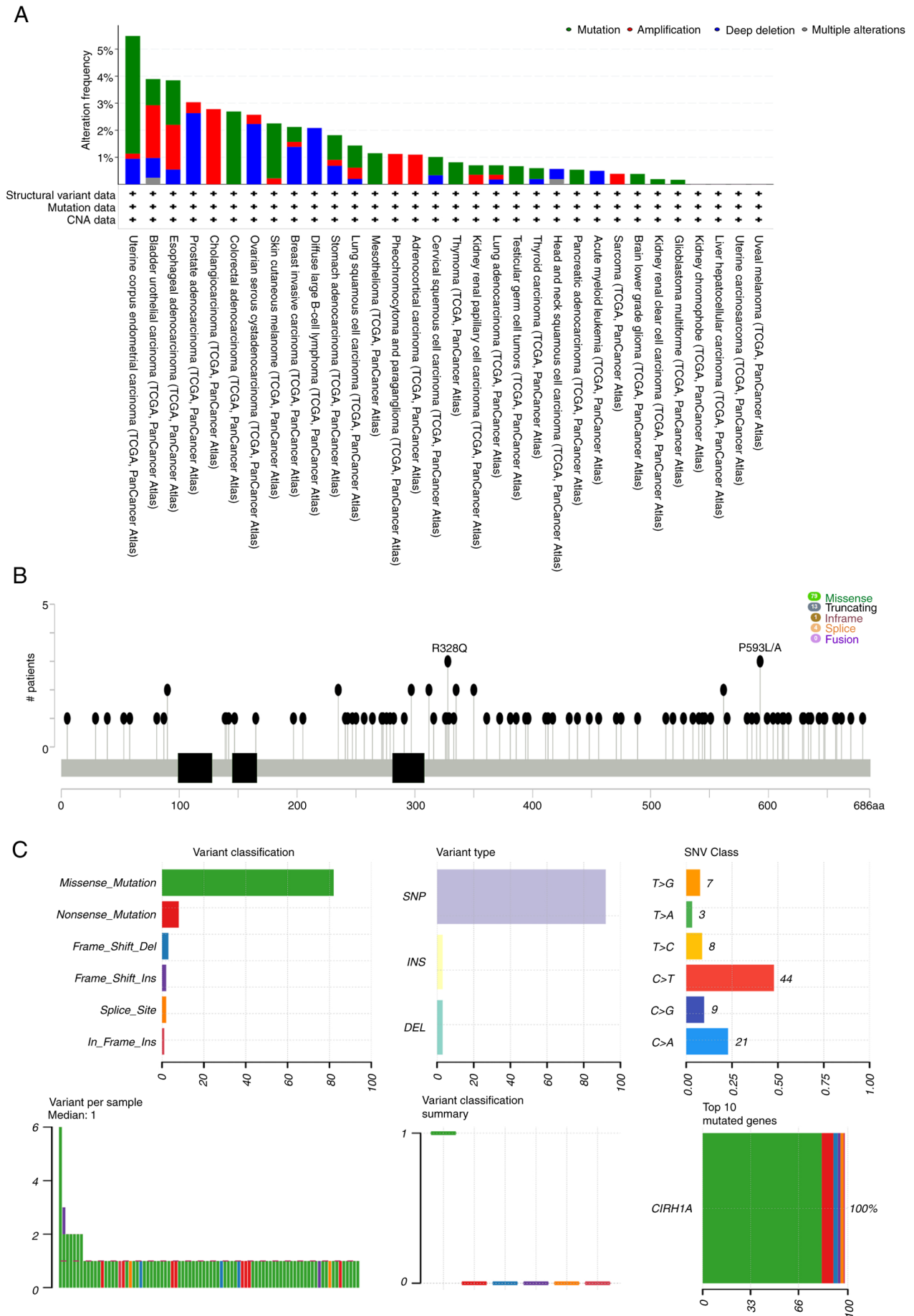


Figure 5. (A) Frequency and alteration types of UTP4 across cancers. (B) Specific mutation sites and mutation types of UTP4 in pan-cancer. (C) Mutation landscape of UTP4 in pan-cancer. TCGA, The Cancer Genome Atlas.

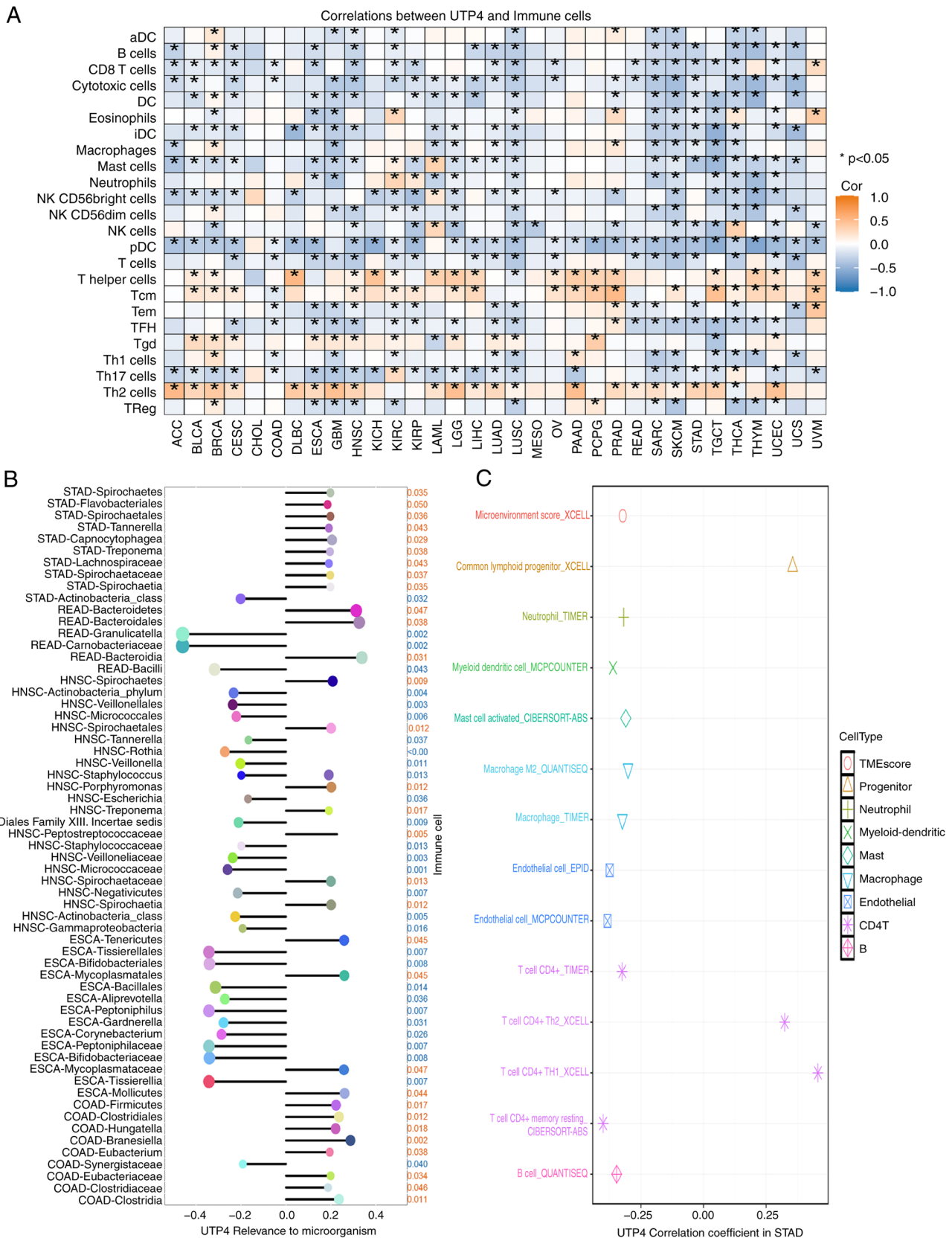


Figure 6. (A) Correlations between UTP4 expression and 24 immune cell types across pan-cancer. *P<0.05. (B) Correlations between UTP4 expression and intra-tumoral microbes in pan-cancer. (C) Correlations between UTP4 and immune cells specifically in gastric cancer. ACC, adenoid cystic carcinoma; BLCA, bladder urothelial carcinoma; BRCA, breast cancer; CESC, cervical squamous cell carcinoma; CHOL, cholangiocarcinoma; COAD, colon adenocarcinoma; DLBC, diffuse large B-cell lymphoma; ESCA, esophageal carcinoma; GBM, glioblastoma multiforme; HNSC, head and neck cancer; KICH, kidney chromophobe; KIRC, kidney renal clear cell carcinoma; KIRP, kidney renal papillary carcinoma; LAML, acute myeloid leukemia; LGG, low-grade glioma; LHC, liver hepatocellular carcinoma; LUAD, lung adenocarcinoma; LUSC, lung squamous cell carcinoma; MESO, mesothelioma; OV, ovarian cancer; PAAD, pancreatic adenocarcinoma; PCPG, pheochromocytoma; PRAD, prostate adenocarcinoma; READ, rectum adenocarcinoma; SARC, sarcoma; SKCM, skin cutaneous melanoma; STAD, stomach adenocarcinoma; TGCT, tenosynovial giant cell tumor; THCA, thyroid carcinoma; THYM, thymoma; UCEC, uterine corpus endometrial carcinoma; UCS, uterine carcinosarcoma; UVM, uveal melanoma.

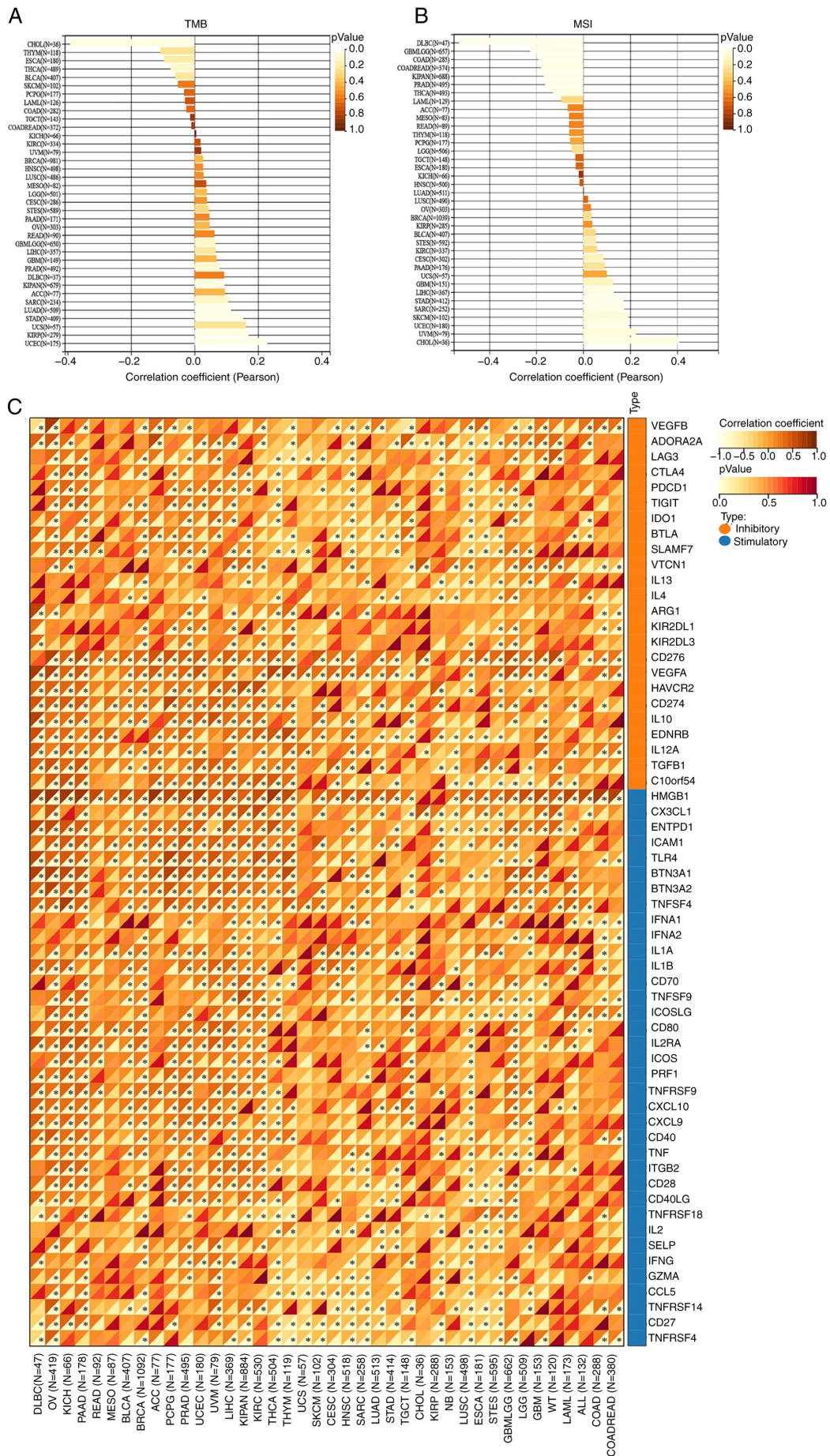


Figure 7. (A and B) Bar charts illustrating correlations between UTP4 expression and TMB and MSI across pan-cancer. (C) Heatmap of correlation analysis between UTP4 and two types of immune checkpoint marker genes (*P<0.05). TMB, tumor mutational burden; MSI, microsatellite instability.

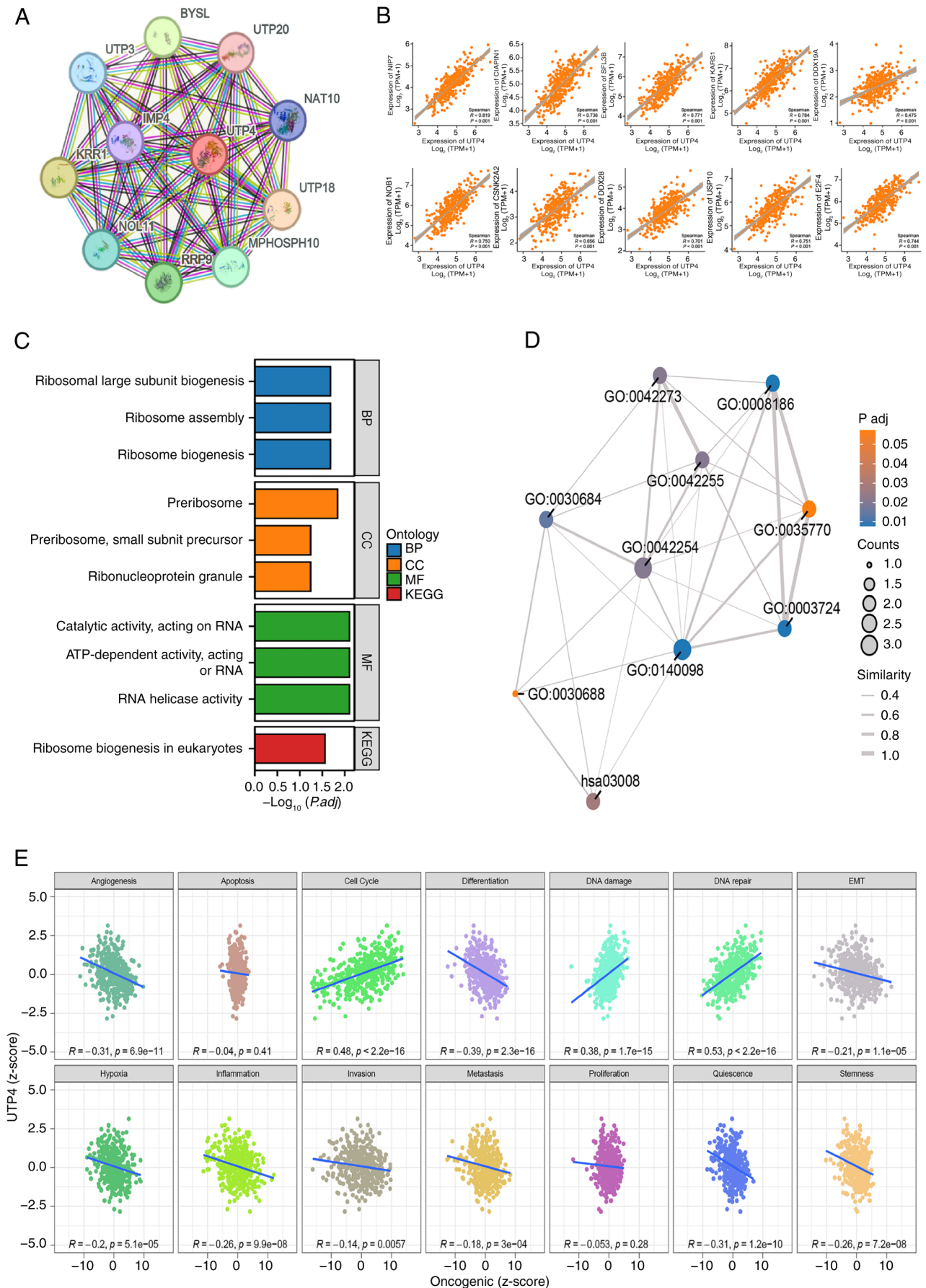


Figure 8. (A) Protein-protein interaction network of UTP4 from the STRING database. (B) Scatter plots depicting the top 10 genes correlated with UTP4 (shaded area indicates 95% confidence interval). (C and D) Bar charts and enrichment map (EMAP) illustrating GO/KEGG enrichment analyses for genes related to CCDC58. (E) Pearson correlation between UTP4 expression z-scores and GSEA scores of 14 tumor state parameters in stomach adenocarcinoma. GO, Gene Ontology; KEGG, Kyoto Encyclopedia of Genes and Genomes; BP, biological processes; CC, cellular components; MF, molecular functions.

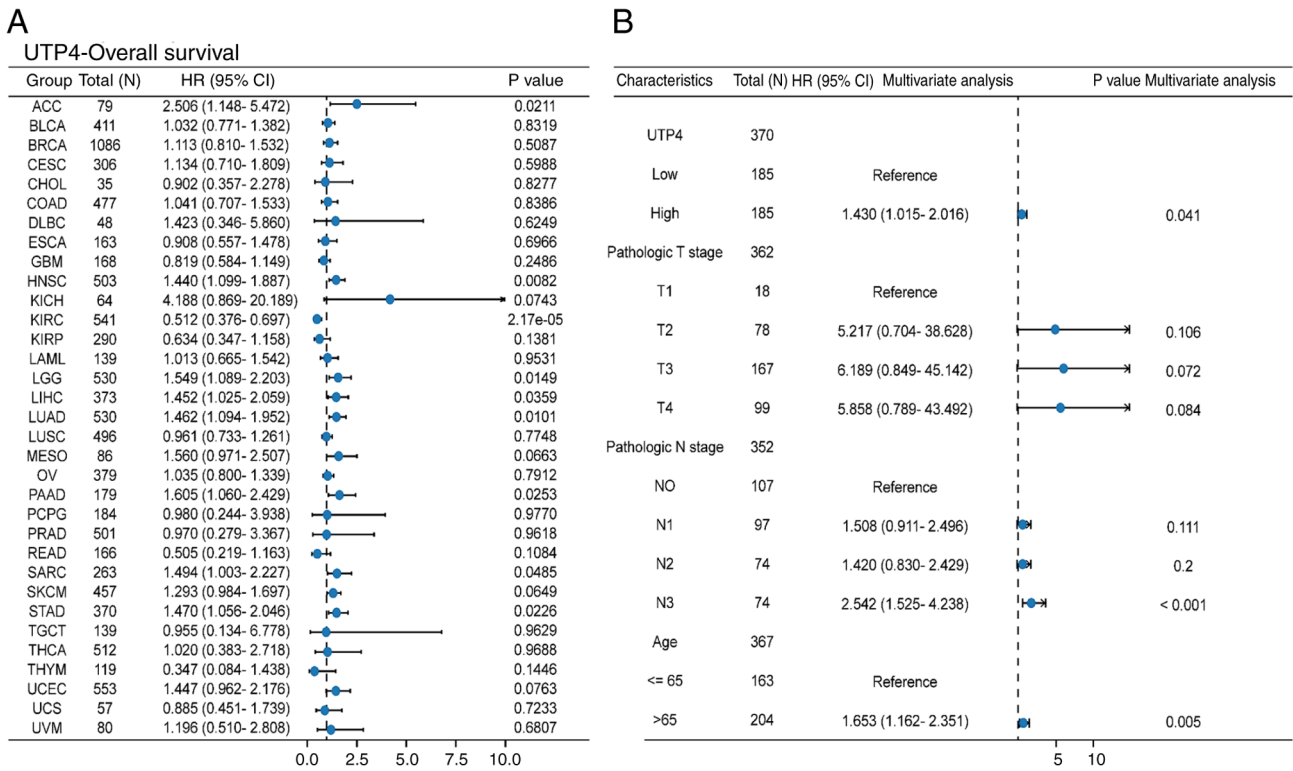


Figure 9. (A) Forest plot of univariate Cox regression analysis results for UTP4 across pan-cancer. (B) Forest plot of multivariate Cox regression analysis results for GC (STAD), including variables pathological T stage, pathological N stage, age and 'UTP4 expression level'. ACC, adenoid cystic carcinoma; BLCA, bladder urothelial carcinoma; BRCA, breast cancer; CESC, cervical squamous cell carcinoma; CHOL, cholangiocarcinoma; COAD, colon adenocarcinoma; DLBC, diffuse large B-cell lymphoma; ESCA, esophageal carcinoma; GBM, glioblastoma multiforme; HNSC, head and neck cancer; KICH, kidney chromophobe; KIRC, kidney renal clear cell carcinoma; KIRP, kidney renal papillary carcinoma; LAML, acute myeloid leukemia; LGG, low-grade glioma; LIHC, liver hepatocellular carcinoma; LUAD, lung adenocarcinoma; LUSC, lung squamous cell carcinoma; MESO, mesothelioma; OV, ovarian cancer; PAAD, pancreatic adenocarcinoma; PCPG, pheochromocytoma; PRAD, prostate adenocarcinoma; READ, rectum adenocarcinoma; SARC, sarcoma; SKCM, skin cutaneous melanoma; STAD, stomach adenocarcinoma; TGCT, tenosynovial giant cell tumor; THCA, thyroid carcinoma; THYM, thymoma; UCEC, uterine corpus endometrial carcinoma; UCS, uterine carcinosarcoma; UVM, uveal melanoma.

In GC, Pearson correlation analysis between UTP4 expression z-scores and GSVA scores of 14 tumor states showed significant positive correlations with the cell cycle, DNA damage and DNA repair ($P < 0.05$; Fig. 8E). This suggests that UTP4 may facilitate cell proliferation and tumor progression, and its elevated expression might indicate increased DNA damage coupled with active repair mechanisms in tumor cells. Conversely, UTP4 expression negatively correlated with angiogenesis, differentiation, epithelial-mesenchymal transition, hypoxia, inflammation, quiescence and stemness. However, the precise roles of UTP4 in these states require further investigation.

Prognostic univariate and multivariate Cox regression. To assess the prognostic significance of UTP4, pan-cancer univariate and GC multivariate Cox regression analyses were performed using RNA-seq data and clinical information from 33 cancer types (TCGA database). Univariate analysis revealed that UTP4 significantly influenced patient prognosis in ACC ($P = 0.0211$), HNSC ($P = 0.0082$), KIRC ($P = 2.17 \times 10^{-5}$), LGG ($P = 0.0149$), LIHC ($P = 0.0359$), LUAD ($P = 0.0101$), PAAD ($P = 0.0253$), SARC ($P = 0.0485$) and STAD ($P = 0.0226$) (Fig. 9A). These findings indicate the potential utility of UTP4 as a prognostic biomarker across multiple cancers.

Subsequently, multivariate Cox regression was performed for GC (STAD), including clinical variables (pathological T stage, pathological N stage, age) with P -values < 0.1 from univariate analyses along with UTP4 expression. The results demonstrated that UTP4 expression remained statistically significant ($P = 0.041$) after adjusting for clinical factors (Fig. 9B), further validating UTP4 as an independent prognostic factor in GC.

Colocalization analysis of UTP4 in pan-cancer and GC. Colocalization analysis evaluates genetic associations between genes and disease-related SNPs to elucidate potential disease mechanisms (33). Colocalization of UTP4 with pan-cancer GWAS data identified the locus rs74886619, displaying a posterior probability of 1 (Fig. 10A). This result indicates potential shared genetic mechanisms between UTP4 and pan-cancer, emphasizing its importance. Similarly, in GC (STAD), colocalization analysis identified rs113952386 with a posterior probability of 0.87 (Fig. 10B), suggesting a significant genetic role for UTP4 in GC development.

Gene editing-CRISPR-Cas9 CERES growth essentiality scores predict the effect of UTP4 knockout. To predict the effect of UTP4 knockout on cancer cell proliferation, CRISPR-Cas9 screening data from the DepMap database

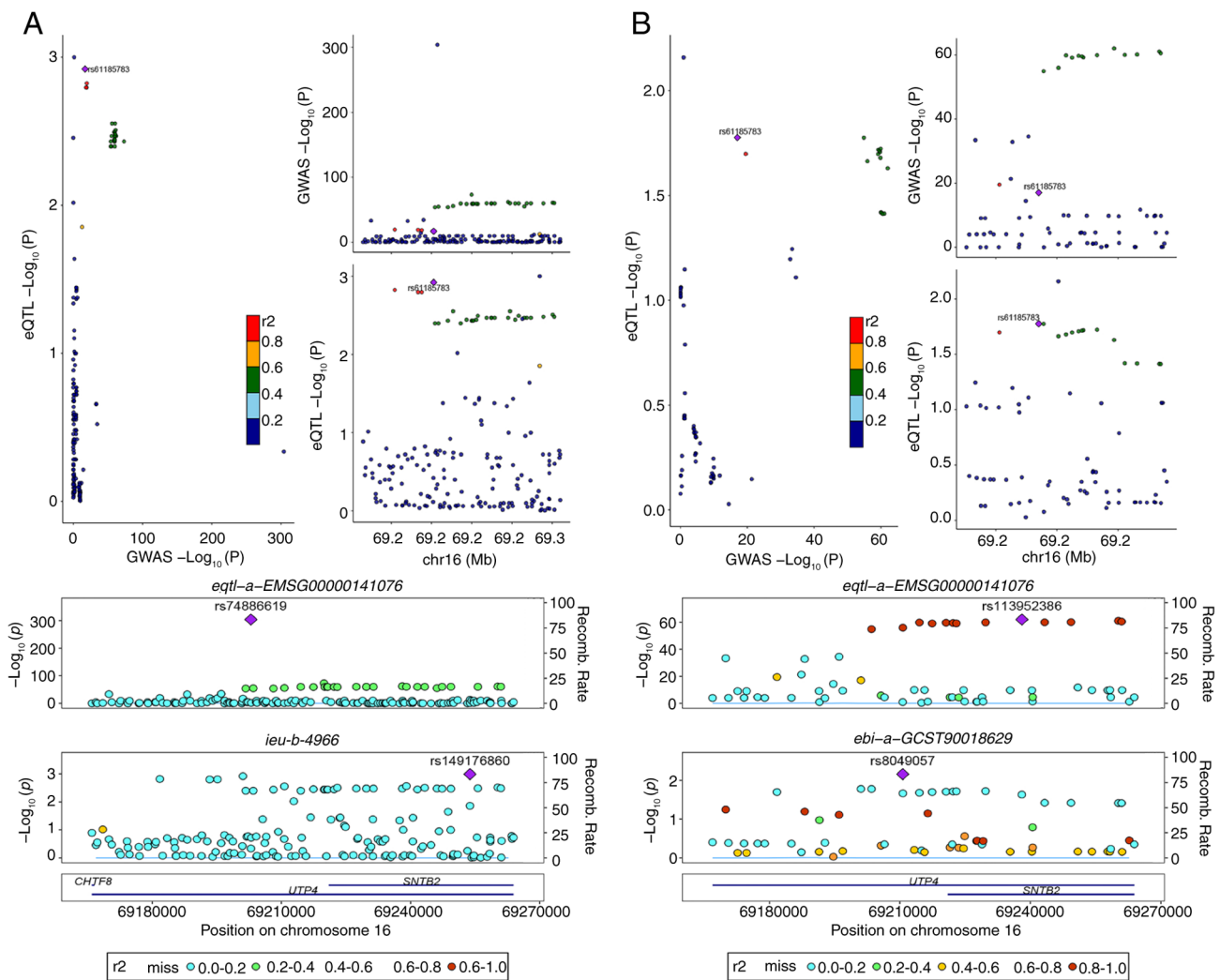


Figure 10. (A) Bayesian colocalization analysis of UTP4 with pan-cancer (ieu-b-4966). (B) Bayesian colocalization analysis of UTP4 with GC (STAD, ebi-a-GCST90018629).

were analyzed to measure gene essentiality (34). Data scaling ensured accurate scoring, with 0 representing non-essential genes and -1 indicating median effects of core essential genes. UTP4 dependency scores were frequently below -1.5, approaching -2 in various cancer cell lines, such as BLCA, BRCA and CESC (Fig. 11). These scores indicate that UTP4 is essential in these cell lines, suggesting that its knockout might significantly inhibit cancer cell proliferation or induce apoptosis, thereby confirming its role in cancer cell proliferation and survival.

UTP4 knockout inhibits proliferation and migration, promotes apoptosis in STAD. Based on genetic associations from colocalization analysis and CRISPR-Cas9 screening predictions, the function of UTP4 in GC cells was further investigated. First, qPCR was employed to evaluate UTP4 mRNA expression in normal gastric epithelial cells (GES-1) and GC cell lines (AGS and MKN-45). UTP4 expression was significantly higher in GC cell lines compared with normal epithelial cells (Fig. 12A). Specific sgRNAs were designed to silence UTP4 expression effectively in both GC cell lines, and the efficacy of the selected sgRNA (sgUTP4#2) was confirmed via qPCR

(Fig. 12B and C). Subsequent CCK-8, wound healing and apoptosis assays showed a marked decrease in proliferation of AGS and MKN-45 cells within 72 hours following UTP4 knockout (Fig. 12D and E). Furthermore, cell migration was significantly reduced after 48 h (Fig. 12F and G). These findings substantiate the critical role of UTP4 in GC cell migration, suggesting its involvement in invasive processes related to cancer progression. Additionally, apoptosis assays revealed a significant increase in apoptosis rates following UTP4 depletion. The apoptosis rate in AGS cells increased notably from 6.93 to 13.4%, and in MKN-45 cells from 16.04 to 28.3% (Fig. 12H and I). These results indicated that UTP4 knockout significantly inhibits GC cell proliferation and migration and promotes apoptosis, validating its critical role in GC biology.

Discussion

Ribosomes are increasingly recognized as critical drug targets and prognostic markers in cancer treatment. Their central roles in protein synthesis, biomolecule assembly and regulation of cell proliferation are closely associated with tumor initiation and progression (35,36). In particular, ribosomes

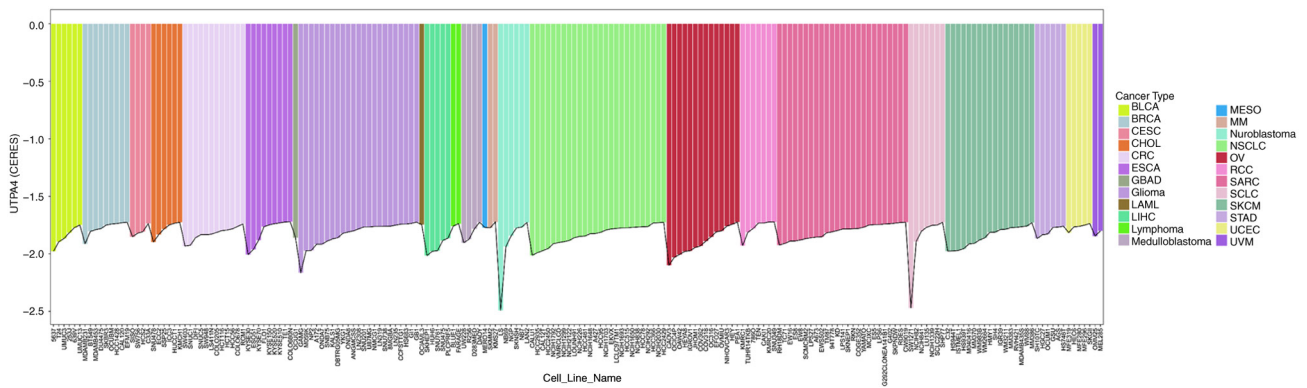


Figure 11. Visualization of CERES growth essentiality scores for UTP4 across the top 200 pan-cancer cell lines (y-axis represents CERES scores; x-axis indicates different cell lines; colors represent different tumor types). BLCA, bladder urothelial carcinoma; BRCA, breast cancer; CESC, cervical squamous cell carcinoma; CHOL, cholangiocarcinoma; CRC, colorectal cancer; ESCA, esophageal carcinoma; GBAD, gallbladder adenocarcinoma; LAML, acute myeloid leukemia; LIHC, liver hepatocellular carcinoma; MESO, mesothelioma; MM, multiple myeloma; NSCLC, non-small cell lung cancer; OV, ovarian cancer; RCC, renal cell carcinoma; SARC, sarcoma; SCLC, small cell lung cancer; SKCM, skin cutaneous melanoma; STAD, stomach adenocarcinoma; UCEC, uterine corpus endometrial carcinoma; UVM, uveal melanoma.

regulate translation initiation, RB, and cellular signaling, making them attractive targets for anticancer therapy (37,38). Ribosome-targeted therapies have effectively suppressed cancer cell proliferation, migration and survival, particularly in drug-resistant tumor cells and cancer stem cells (39,40). For example, specific drugs such as CX-5461 (an RNA polymerase I inhibitor) and GCN2 inhibitors (genome integrity protein kinase 2 inhibitors) block ribosomal RNA synthesis, inhibit protein synthesis, and induce apoptosis in cancer cells (40,41).

UTP4 is essential for pre-ribosomal RNA processing, particularly in the nucleolar maturation of 18S rRNA, and is crucial in RB. Elevated UTP4 expression potentially supports rapid cancer cell proliferation by promoting RB. Moreover, studies indicate that UTP4 may also function as a transcriptional regulator (42). In the present study, the expression patterns and prognostic implications of UTP4 were systematically analyzed across multiple cancers and experimentally confirmed its biological significance in GC.

In the present study, UTP4 expression was initially assessed and validated in GC using RNA and protein data from the TCGA cohort, confirming that UTP4 is significantly upregulated in most cancer types. Single-cell spatial transcriptomic analysis further verified high UTP4 expression in various tumor cell populations. Given the strong prognostic and diagnostic significance of UTP4 identified in the TCGA cohort, its functional mechanisms were explored through multi-omics approaches. Functional analyses indicated that UTP4 gene mutations, mainly missense and nonsense mutations, commonly occur in multiple cancers, potentially influencing UTP4 function and promoting tumorigenesis. Additionally, UTP4 expression negatively correlated with the infiltration of several immune cells but positively correlated with specific populations such as T helper cells, Tcm cells and Th2 cells. This suggests UTP4 may contribute to an immunosuppressive TME, enabling immune evasion. Moreover, high UTP4 expression correlated positively with microbial presence in TMEs, especially in GC and CRC, potentially further accelerating tumor progression. The present findings also indicated that UTP4 may influence cancer progression and metastasis by regulating tumor stemness, mutational burden and immune checkpoint molecules.

Univariate and multivariate regression analyses confirmed that UTP4 serves as an independent prognostic indicator in GC. Bayesian colocalization genetic association analysis and CRISPR-Cas9 predictions further validated UTP4's functional role. The present study further demonstrated that high UTP4 expression was significantly correlated with poor OS but not DFI. This discrepancy suggests UTP4 does not primarily drive initial tumor recurrence; instead, it plays a key role in accelerating disease progression and lethality post-recurrence. Thus, UTP4 mainly acts in advanced disease stages, driving progression and poor outcomes, supporting its potential as a therapeutic target for advanced tumors. Specifically, UTP4 knockdown significantly reduced proliferation and migration while promoting apoptosis in GC cell lines (AGS and MKN-45). These results confirm the pivotal role of UTP4 in GC development, reinforcing its potential as a therapeutic target and prognostic biomarker.

Notably, UTP4 functions not only at the mRNA level but also as a circular RNA (circRNA-CIRH1A), exhibiting significant expression in various cancers associated with cell proliferation, migration and invasion (43,44). CircRNAs commonly act as 'sponges' for specific miRNAs, thus regulating downstream signaling pathways (44,45). For instance, circRNA-CIRH1A influences the PI3K/AKT and JAK2/STAT3 signaling pathways by sponging miR-1276, an interaction validated in osteosarcoma cells (46). These findings suggest that elevated UTP4 expression may affect cancer progression via both protein-coding and circular RNA mechanisms. Therefore, distinguishing whether the cancer-promoting effects of UTP4 are mediated primarily by its mRNA or circRNA form is critical. Although systematic pan-cancer analyses demonstrated that UTP4 mRNA promotes tumorigenesis, the precise roles of its circRNA form remain unclear. A recent study indicated that circular RNAs function as inhibitors or activators influencing GC initiation and progression, emphasizing their potential utility as diagnostic biomarkers and therapeutic targets (47). The experimental findings of the present study clearly demonstrated UTP4's impact on GC cells; however, as the entire UTP4 gene was targeted for knockout, potential effects of

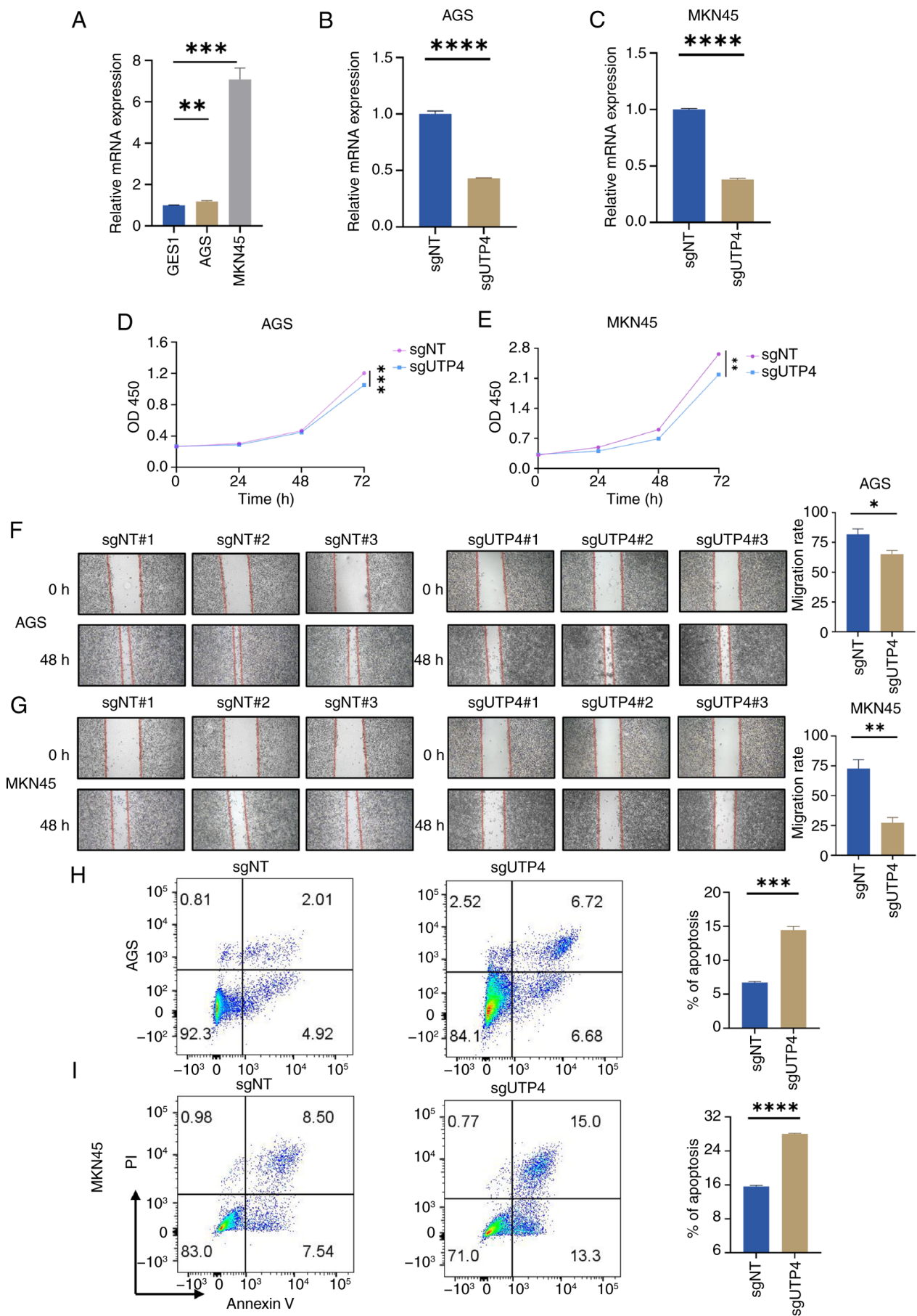


Figure 12. (A) UTP4 mRNA expression levels in GES-1, AGS and MKN-45 cells. (B and C) Validation of UTP4 knockdown efficiency mediated by the selected sgRNA (sgUTP4#2) via qPCR. (D and E) Cell proliferation assays. (F and G) Wound healing assays assessing cell migration. (H and I) Flow cytometric analysis of apoptosis rates in AGS and MKN-45 cells. * $P < 0.05$, ** $P < 0.01$, *** $P < 0.001$ and **** $P < 0.0001$.

its circRNA form cannot be excluded. Clarifying the distinct roles of UTP4 in different RNA forms will provide deeper insights into its diverse functions in cancer biology, opening new avenues for targeted therapeutic development.

Currently, studies linking UTP4 abnormalities to disease are limited, with most studies focused on North American Indian childhood cirrhosis. The role of UTP4 in other diseases remains largely unexplored. Research on UTP4's relationship with cancer is predominantly restricted to CRC, leaving its involvement in other cancers unclear. Studies indicate that cancer cells produce neuroendocrine mediators, activating central neuroendocrine axes and establishing bidirectional communication with autonomic and sensory nerves. This process disrupts metabolic, immune, and circadian homeostasis. UTP4 might facilitate the production of neuroendocrine mediators by enhancing RB, thereby activating central neuroendocrine pathways, regulating immune-metabolic homeostasis, and promoting cancer-related homeostatic disruption (48). Therefore, the present study addresses an existing research gap, has innovative significance, and provides a foundation for future research.

However, the current findings primarily depend on publicly available databases. The inherent batch effect, variations in data quality and sample processing heterogeneity in these databases may introduce biases, impacting the accuracy of UTP4 expression measurements and cross-cancer comparisons. These factors should be taken into consideration when interpreting the findings of the present study and their generalizability. Additionally, non-random sample selection could limit the generalizability of our findings across different populations and cancer subtypes. Therefore, additional clinical data are necessary to confirm the potential of UTP4 as a reliable biomarker. Though the current pan-cancer analysis points to a wide-ranging involvement of UTP4 in tumorigenesis, functional validation has thus far been confined exclusively to GC. Thus, subsequent studies are warranted to verify its functional relevance in other malignancies. The present study is predominantly reliant on analyses of public databases and lacks validation using prospective clinical cohorts or fresh tissue samples, which represents a major barrier to its clinical translation. Furthermore, the current functional evidence remains insufficient: The absence of *in vivo* data, particularly from murine models, greatly impairs the rigorous validation of UTP4's role in tumorigenesis and therapeutic response. Therefore, future studies should integrate animal model experiments and clinical sample validation to fully confirm its translational potential.

In conclusion, UTP4 exhibits high expression across various cancers and correlates significantly with prognosis in multiple cancer types, including GC. Its expression shows notable associations with TMB, MSI, immune checkpoints, immune cells and microorganisms in a pan-cancer context. *In vitro* experiments validated the oncogenic function of UTP4 in GC cells, further supporting its value as a prognostic biomarker.

Acknowledgements

Not applicable.

Funding

The present study was supported by the Special Project of Science and Technology Cooperation between Hubei and Chinese Academy of Sciences (grant no. 4200002181 7T300000050), the Teaching research project of Medical Faculty of Wuhan University in 2021 (grant no. 2021026) and Wuhan Medical Scientific Research Project (grant no. WX23Q12).

Availability of data and materials

The data generated in the present study may be requested from the corresponding author.

Authors' contributions

DW and QH designed the research. DW, TL and YC analyzed the data and wrote the manuscript. All authors read and approved the final version of the manuscript. DW and QH confirm the authenticity of all the raw data.

Ethics approval and consent to participate

Not applicable.

Patient consent for publication

Not applicable.

Competing interests

The authors declare that they have no competing interests.

References

- Vishwanath A, Krishna S, Manudhane AP, Hart PA and Krishna SG: Early-onset gastrointestinal malignancies: An investigation into a rising concern. *Cancers (Basel)* 16: 1553, 2024.
- López MJ, Carbajal J, Alfaro AL, Saravia LG, Zanabria D, Araujo JM, Quispe L, Zevallos A, Buleje JL, Cho CE, *et al*: Characteristics of gastric cancer around the world. *Crit Rev Oncol Hematol* 181: 103841, 2023.
- Smyth EC, Nilsson M, Grabsch HI, van Grieken NC and Lordick F: Gastric cancer. *Lancet* 396: 635-648, 2020.
- Boilève J, Toucheffeu Y and Matysiak-Budnik T: Clinical management of gastric cancer treatment regimens. *Curr Top Microbiol Immunol* 444: 279-304, 2023.
- Li S, Gao J, Xu Q, Zhang X, Huang M, Dai X, Huang K and Liu L: A signature-based classification of gastric cancer that stratifies tumor immunity and predicts responses to PD-1 inhibitors. *Front Immunol* 12: 693314, 2021.
- Lordick F, Carneiro F, Cascinu S, Fleitas T, Haustermans K, Piessen G, Vogel A and Smyth EC; ESMO Guidelines Committee. Electronic address: clinicalguidelines@esmo.org; Gastric cancer: ESMO clinical practice guideline for diagnosis, treatment and follow-up. *Ann Oncol* 33: 1005-1020, 2022.
- Kang YK, Boku N, Satoh T, Ryu MH, Chao Y, Kato K, Chung HC, Chen JS, Muro K, Kang WK, *et al*: Nivolumab in patients with advanced gastric or gastro-oesophageal junction cancer refractory to, or intolerant of, at least two previous chemotherapy regimens (ONO-4538-12, ATTRACTION-2): A randomised, double-blind, placebo-controlled, phase 3 trial. *Lancet* 390: 2461-2471, 2017.
- Yasuda T and Wang YA: Gastric cancer immunosuppressive microenvironment heterogeneity: Implications for therapy development. *Trends Cancer* 10: 627-642, 2024.

9. Kim R, An M, Lee H, Mehta A, Heo YJ, Kim KM, Lee SY, Moon J, Kim ST, Min BH, *et al*: Early tumor-immune microenvironmental remodeling and response to first-line fluoropyrimidine and platinum chemotherapy in advanced gastric cancer. *Cancer Discov* 12: 984-1001, 2022.
10. Calviño FR, Kornprobst M, Schermann G, Birkle F, Wild K, Fischer T, Hurt E, Ahmed YL and Sinning I: Structural basis for 5'-ETS recognition by Utp4 at the early stages of ribosome biogenesis. *PLoS One* 12: e0178752, 2017.
11. Wang C, Ma H, Baserga SJ, Pederson T and Huang S: Nucleolar structure connects with global nuclear organization. *Mol Biol Cell* 34: ar114, 2023.
12. Freed EF and Baserga SJ: The C-terminus of Utp4, mutated in childhood cirrhosis, is essential for ribosome biogenesis. *Nucleic Acids Res* 38: 4798-4806, 2010.
13. Wilkins BJ, Lorent K, Matthews RP and Pack M: p53-mediated biliary defects caused by knockdown of *cirh1a*, the zebrafish homolog of the gene responsible for North American Indian childhood cirrhosis. *PLoS One* 8: e77670, 2013.
14. Guo F, Chen JJ and Tang WJ: CIRH1A augments the proliferation of RKO colorectal cancer cells. *Oncol Rep* 37: 2375-2381, 2017.
15. Gahoi N, Syed P, Choudhary S, Epari S, Moiyadi A, Varma SG, Gandhi MN and Srivastava S: A protein microarray-based investigation of cerebrospinal fluid reveals distinct autoantibody signature in low and high-grade gliomas. *Front Oncol* 10: 543947, 2020.
16. Hanley JA and McNeil BJ: The meaning and use of the area under a receiver operating characteristic (ROC) curve. *Radiology* 143: 29-36, 1982.
17. Szklarczyk D, Gable AL, Lyon D, Junge A, Wyder S, Huerta-Cepas J, Simonovic M, Doncheva NT, Morris JH, Bork P, *et al*: STRING v11: Protein-protein association networks with increased coverage, supporting functional discovery in genome-wide experimental datasets. *Nucleic Acids Res* 47: D607-D613, 2019.
18. Tang Z, Li C, Kang B, Gao G, Li C and Zhang Z: GEPIA: A web server for cancer and normal gene expression profiling and interactive analyses. *Nucleic Acids Res* 45: W98-W102, 2017.
19. Hänzelmann S, Castelo R and Guinney J: GSEA: Gene set variation analysis for microarray and RNA-seq data. *BMC Bioinformatics* 14: 7, 2013.
20. Giambartolomei C, Vukcevic D, Schadt EE, Franke L, Hingorani AD, Wallace C and Plagnol V: Bayesian test for colocalisation between pairs of genetic association studies using summary statistics. *PLoS Genet* 10: e1004383, 2014.
21. Livak KJ and Schmittgen TD: Analysis of relative gene expression data using real-time quantitative PCR and the $2^{-\Delta\Delta C(T)}$ method. *Methods* 25: 402-408, 2001.
22. Longo SK, Guo MG, Ji AL and Khavari PA: Integrating single-cell and spatial transcriptomics to elucidate intercellular tissue dynamics. *Nat Rev Genet* 22: 627-644, 2021.
23. Rodrigues SG, Stickels RR, Goeva A, Martin CA, Murray E, Vanderburg CR, Welch J, Chen LM, Chen F and Macosko EZ: Slide-seq: A scalable technology for measuring genome-wide expression at high spatial resolution. *Science* 363: 1463-1467, 2019.
24. Ståhl PL, Salmén F, Vickovic S, Lundmark A, Navarro JF, Magnusson J, Giacomello S, Asp M, Westholm JO, Huss M, *et al*: Visualization and analysis of gene expression in tissue sections by spatial transcriptomics. *Science* 353: 78-82, 2016.
25. Brookes AJ: The essence of SNPs. *Gene* 234: 177-186, 1999.
26. Vignal A, Milan D, SanCristobal M and Eggen A: A review on SNP and other types of molecular markers and their use in animal genetics. *Genet Sel Evol* 34: 275-305, 2002.
27. Reya T, Morrison SJ, Clarke MF and Weissman IL: Stem cells, cancer, and cancer stem cells. *Nature* 414: 105-111, 2001.
28. Clevers H: The cancer stem cell: Premises, promises and challenges. *Nat Med* 17: 313-319, 2011.
29. O'Brien CA, Kreso A and Jamieson CH: Cancer stem cells and self-renewal. *Clin Cancer Res* 16: 3113-3120, 2010.
30. Klinge S and Woolford JL Jr: Ribosome assembly coming into focus. *Nat Rev Mol Cell Biol* 20: 116-131, 2019.
31. Henras AK, Plisson-Chastang C, O'Donohue MF, Chakraborty A and Gleizes PE: An overview of pre-ribosomal RNA processing in eukaryotes. *Wiley Interdiscip Rev RNA* 6: 225-242, 2015.
32. Anderson P and Kedersha N: RNA granules: Post-transcriptional and epigenetic modulators of gene expression. *Nat Rev Mol Cell Biol* 10: 430-436, 2009.
33. Beesley J, Sivakumaran H, Moradi Marjaneh M, Shi W, Hillman KM, Kaufmann S, Hussein N, Kar S, Lima LG, Ham S, *et al*: eQTL colocalization analyses identify NTN4 as a candidate breast cancer risk gene. *Am J Hum Genet* 107: 778-787, 2020.
34. Meyers RM, Bryan JG, McFarland JM, Weir BA, Sizemore AE, Xu H, Dharia NV, Montgomery PG, Cowley GS, Pantel S, *et al*: Computational correction of copy number effect improves specificity of CRISPR-Cas9 essentiality screens in cancer cells. *Nat Genet* 49: 1779-1784, 2017.
35. Pecoraro A, Pagano M, Russo G and Russo A: Ribosome biogenesis and cancer: Overview on ribosomal proteins. *Int J Mol Sci* 22: 5496, 2021.
36. Xu X, Xiong X and Sun Y: The role of ribosomal proteins in the regulation of cell proliferation, tumorigenesis, and genomic integrity. *Sci China Life Sci* 59: 656-672, 2016.
37. Elhamamsy AR, Metge BJ, Alsheikh HA, Shevde LA and Samant RS: Ribosome biogenesis: A central player in cancer metastasis and therapeutic resistance. *Cancer Res* 82: 2344-2353, 2022.
38. Jiao L, Liu Y, Yu XY, Pan X, Zhang Y, Tu J, Song YH and Li Y: Ribosome biogenesis in disease: New players and therapeutic targets. *Signal Transduct Target Ther* 8: 15, 2023.
39. Pelletier J, Thomas G and Volarević S: Ribosome biogenesis in cancer: New players and therapeutic avenues. *Nat Rev Cancer* 18: 51-63, 2018.
40. Bywater MJ, Poortinga G, Sanij E, Hein N, Peck A, Cullinane C, Wall M, Cluse L, Drygin D, Anderes K, *et al*: Inhibition of RNA polymerase I as a therapeutic strategy to promote cancer-specific activation of p53. *Cancer Cell* 22: 51-65, 2012.
41. Kato Y, Kunimasa K, Takahashi M, Harada A, Nagasawa I, Osawa M, Sugimoto Y and Tomida A: GZD824 inhibits GCN2 and sensitizes cancer cells to amino acid starvation stress. *Mol Pharmacol* 98: 669-676, 2020.
42. Freed EF, Prieto JL, McCann KL, McStay B and Baserga SJ: NOL11, implicated in the pathogenesis of North American Indian childhood cirrhosis, is required for pre-rRNA transcription and processing. *PLoS Genet* 8: e1002892, 2012.
43. Memczak S, Jens M, Elefsinioti A, Torti F, Krueger J, Rybak A, Maier L, Mackowiak SD, Gregersen LH, Munschauer M, *et al*: Circular RNAs are a large class of animal RNAs with regulatory potency. *Nature* 495: 333-338, 2013.
44. Hansen TB, Jensen TI, Clausen BH, Bramsen JB, Finsen B, Damgaard CK and Kjems J: Natural RNA circles function as efficient microRNA sponges. *Nature* 495: 384-388, 2013.
45. Hollensen AK, Andersen S, Hjorth K, Bak RO, Hansen TB, Kjems J, Aagaard L, Damgaard CK and Mikkelsen JG: Enhanced tailored MicroRNA sponge activity of RNA Pol II-transcribed TuD hairpins relative to ectopically expressed *ciRS7*-derived circRNAs. *Mol Ther Nucleic Acids* 13: 365-375, 2018.
46. Zhang M, Wang X, Zhao J, Yan J, He X, Qin D, Liang F, Tong K and Wang J: CircRNA-CIRH1A promotes the development of osteosarcoma by regulating PI3K/AKT and JAK2/STAT3 signaling pathways. *Mol Biotechnol* 66: 2241-2253, 2024.
47. Bakhti SZ, Latifi-Navid S, Pahlevan AD, Sarabi L and Safaralizadeh R: The role of circular RNAs in gastric cancer: Focusing on autophagy, EMT, and their crosstalk. *Biochem Biophys Rep* 48: 102169, 2025.
48. Slominski RM, Raman C, Chen JY and Slominski AT: How cancer hijacks the body's homeostasis through the neuroendocrine system. *Trends Neurosci* 46: 263-275, 2023.

